Experimental Investigation on the Crack Closure Duration of Cu-Al-Mn Shape Memory Alloy Reinforced in Al Matrix

Naresh H

Assistant professor, Department of Mechanical Engineering, Siddaganga Institute of Technology, tumakuru – 572103

Abstract

For this study, Cu-Al-Mn shape memory alloys with 10-14.5 wt. % of Al, 0-10 wt. % of Mn and 70-85 wt. % of Cu were chosen. These alloy's superelasticity, shape memory effect, and transition temperatures are all extremely sensitive to changes in composition. By using differential scanning calorimetry, bend and tensile tests, it has been possible to better understand how composition affects these properties. It is discovered that the shape of martensite and its transformation temperatures alter as the amount of aluminium increases. As manganese content rises, however, martensite is stabilised and the alloy's superelasticity is improved.

Keywords: Shape memory alloy; Materials; Shape recovery; Alloy.

1. Introduction

Due to their unusual characteristics, such as the shape memory effect, pseudo-elasticity or large recoverable strain, high damping capacity, and adaptive properties, which are caused by the (reversible) phase transitions in the materials, shape memory alloys (SMAs) are one of the main components of intelligent/smart composites [1]. Application of materials naturally results in degradation, damage, and failure. Though all engineered materials eventually fail, engineering research has historically been concentrated on either the design of new materials with higher robustness or the development of non-destructive evaluation methods for material inspection to any of the aforementioned flaws. Researchers are looking towards self-healing materials that can fix damage as a result of the aforementioned issues. Self-healing materials go through three processes in order to repair themselves. Injury causes the initial response to occur. The second response is the delivery of supplies to the damaged area, and the chemical repair process which is comparable to matrix remodelling is the third response. One of the current healing techniques that can make the fibre reinforced polymer composites healable is the hollow glass fibre (HGF) healing system. These HGFs are created in a glass workshop utilising the hollow glass drawing process. In composite structures, a typical HGF self-healing method can involve fibres that contain a one-part resin system, a two-part resin and hardener system, or a resin system with a catalyst or hardener built right into the matrix material. It is preferable to store the healing ingredient in hollow fibres rather than microcapsules in composites [2]. It is generally known that damage to oxide layers, which typically prevent the surfaces of metals like aluminium (Al) and titanium (Ti) from corroding, can be restored by re-oxidation in air, which can be viewed as a type of self-repair, when it comes to metals and other inanimate materials. Currently, research is focused on procedures that could potentially repair flaws like cracks that can appear inside materials during production or during use. These self-healing mechanisms might then enable the prevention of failures and an extension of the useful lives of parts and structures. On the macro, micro, or nano atomic sizes, materials can self-heal. One of the best examples of the mechanisms that may be exploited for self-healing at the macro level is the sintering of metal particles to create a solid body. The processes at the other end of the spectrum, like dynamic precipitation, which can immobilise dislocations and other flaws in an alloy when it is loaded, only entail localised movement of atoms. Evidence is mounting that small internal fissures can self-heal at the intermediate or micro level [3]. Polymers and polymer matrix composites (PMCs), which are quickly replacing their metal, ceramic, and wood equivalents, have seen a tremendous increase in use over the past 50 years. Despite the fact that the exponential expansion of composites in the aerospace business appears to be a positive microcosm for the ongoing growth of the polymer industry as a whole, issues occur when combining different material types that have essentially diverse failure behaviours. The traditional strategy to regulating damage and engineering materials to better withstand thermal and mechanical loads is used to prevent failure in PMCs [4]. A high symmetry parent phase (austenite) and a low symmetry product phase undergo a thermo-elastic crystalline phase change, which results in the shape memory behaviour (martensite). This change can be undone and depends on both temperature and stress. The crystallographic twins will reorient to the specific form that is preferred by the direction of the load if the martensitic structure is

mechanically stressed at constant temperature. This process is known as reorientation and causes a macroscopic strain [5].

2. Experimental work

2.1. Casting of shape memory alloy Cu-Al 10.54 wt. % and Mn-8.52 wt. %
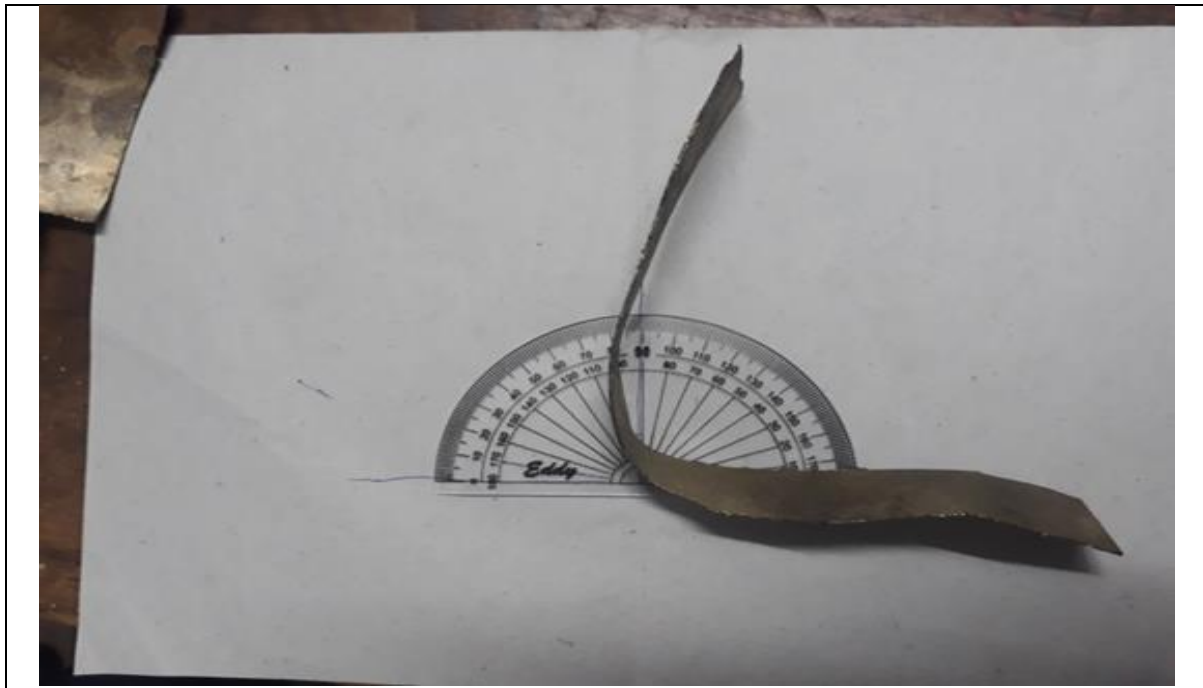

(a)

(b)

(c)

(d)

(e)

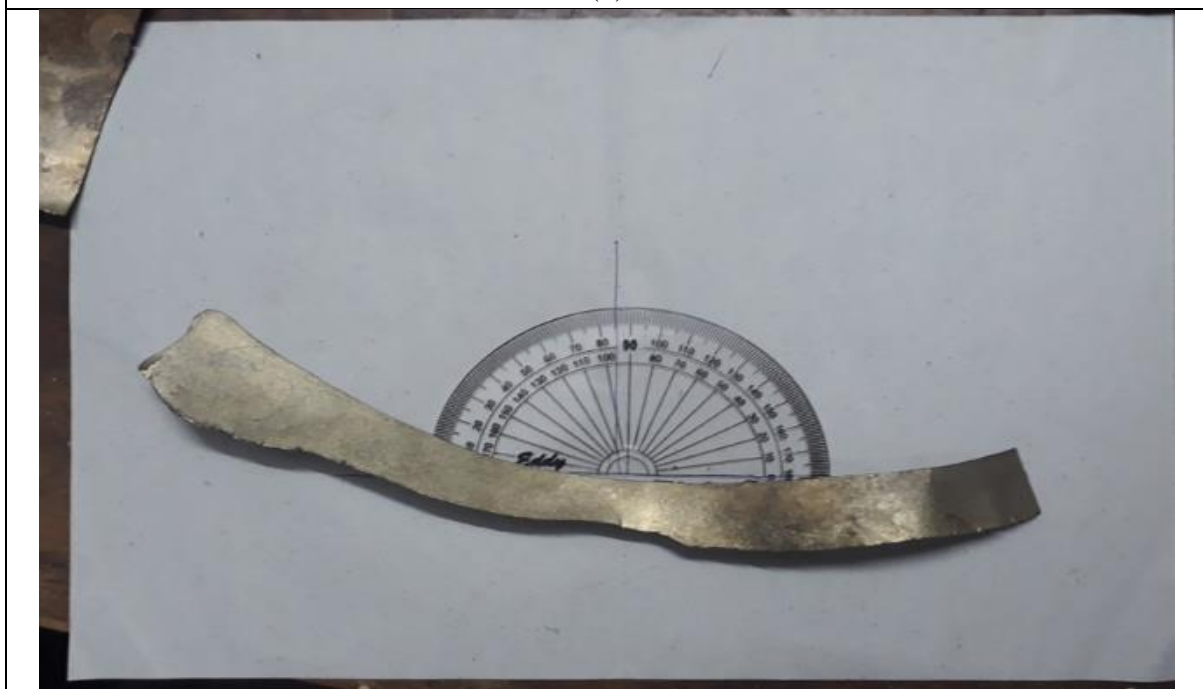Figure-1. Photographic view of casting process

2.2. Percentage of shape recovery (strains)

(a)

(b)

(c)

Figure-2. Photographic view of shape recovery strains

2.3. Constructed frame for holding fibres with some pre-tension

Figure-3. Photographic view of frame constructed for holding wire for reinforcing with Al matrix

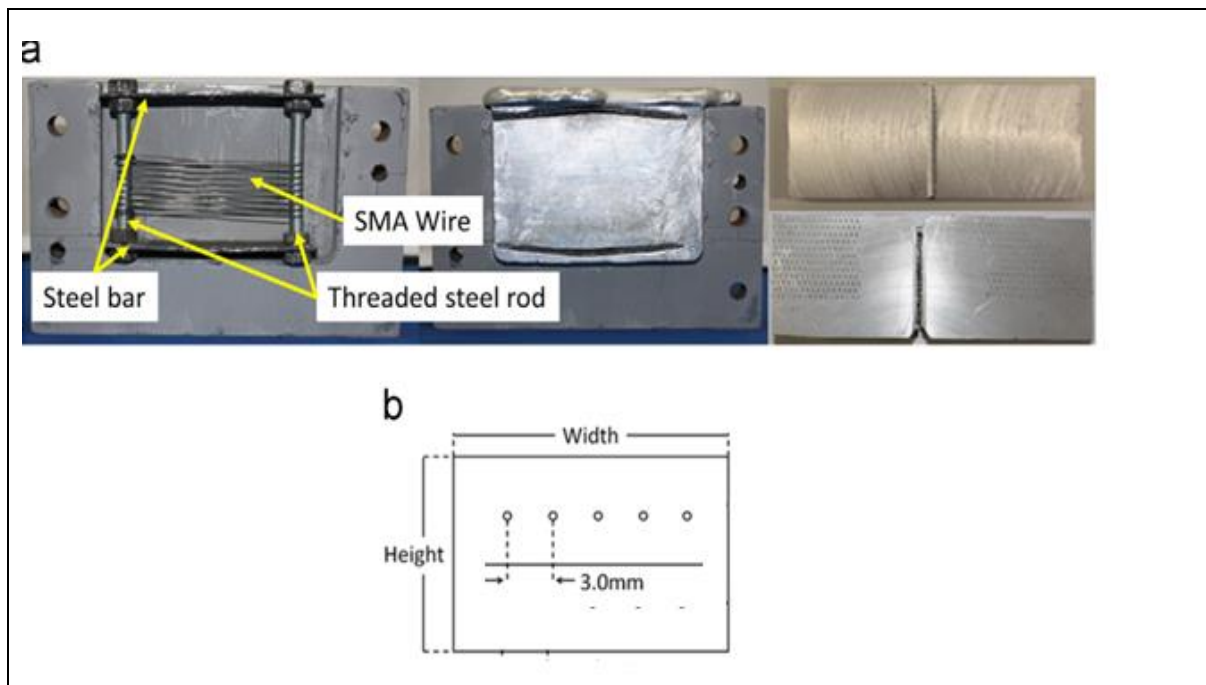## 2.4. Wire of diameter 0.8 mm is drawn for reinforcing with Al matrix

Figure-4. (a) Synthesis of Cu-Al-Mn SMA (left and centre) notched before and after cracking sample (right). (b) Schematic of reinforcement arrangement.

3. Results and discussion

3.1. Compositional analysis

The alloys composition plays a key role in determining the SMAs transformation temperatures and other characteristics. The composition range of the alloys was chosen that they exhibit β-phase at higher temperatures and manifest shape memory effect on quenching to form martensite. From the literature survey it is found that, if there is an increase in manganese and aluminium concentrations of the alloy, the transformation temperature temperatures decrease and if there is an increase in the aluminium content decreases the superelasticity. So 10-14.5 wt. % of Al, 0-10 wt. % of Mn and 70- 85 wt. % of Cu were chosen as the composition range of alloys. The present study used composition range as follows.

Copper (Cu) – 79.21 wt. %, Aluminium (Al) – 11.10 wt. %, and Manganese (Mn) – 7.89 wt. %

3.2. Percentage of shape recovery

$\theta_M = 80°$ (angle recover after heating)

$\theta_E = 90°$ (angle recover after unloading)

SME percentage $= \theta_M / (180 – \theta_E)$

$$= 80 / (180 – 90)$$

SME percentage = 88.88%.

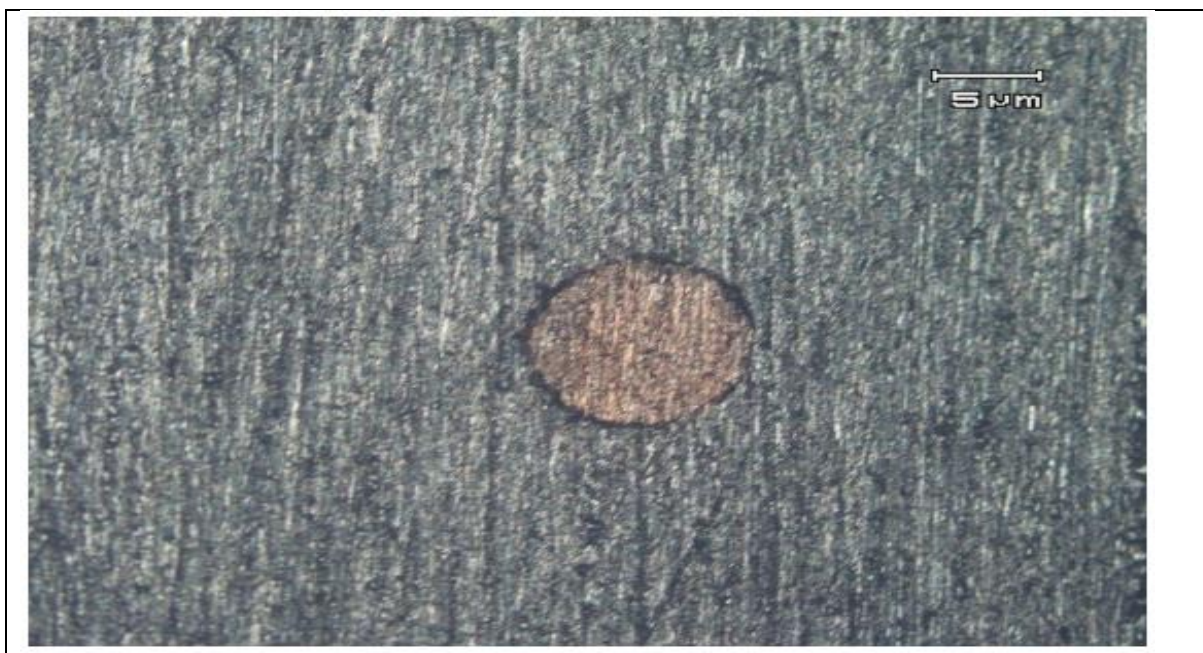### 3.3. Microstructure of region surrounding SMA wire

Figure-5. Optical micrograph of region surrounding Cu-Mn-Al SMA wire

Figure-5 shows the region around the Cu-Mn-Al SMA wire. Between matrix aluminium and the Cu-Mn-Al SMA wire there is a poor bonding. The poor bonding between the SMA wire and aluminium matrix is due to compressive residual stress in the aluminium matrix of SMA wire reinforced composite that can be induced by thermo-mechanical process. This is slightly due to the co-efficient of thermal expansion mismatch between the SMA wire reinforcement and the matrix aluminium and slightly due to the reinforced SMA wire shrinkage during the reverse transformation upon heating to above the Af temperature. When oxidation occurs about 1-µm- thick interfacial layer is formed, resulting in poor bonding between aluminium matrix and Cu-Mn-Al SMA wire.
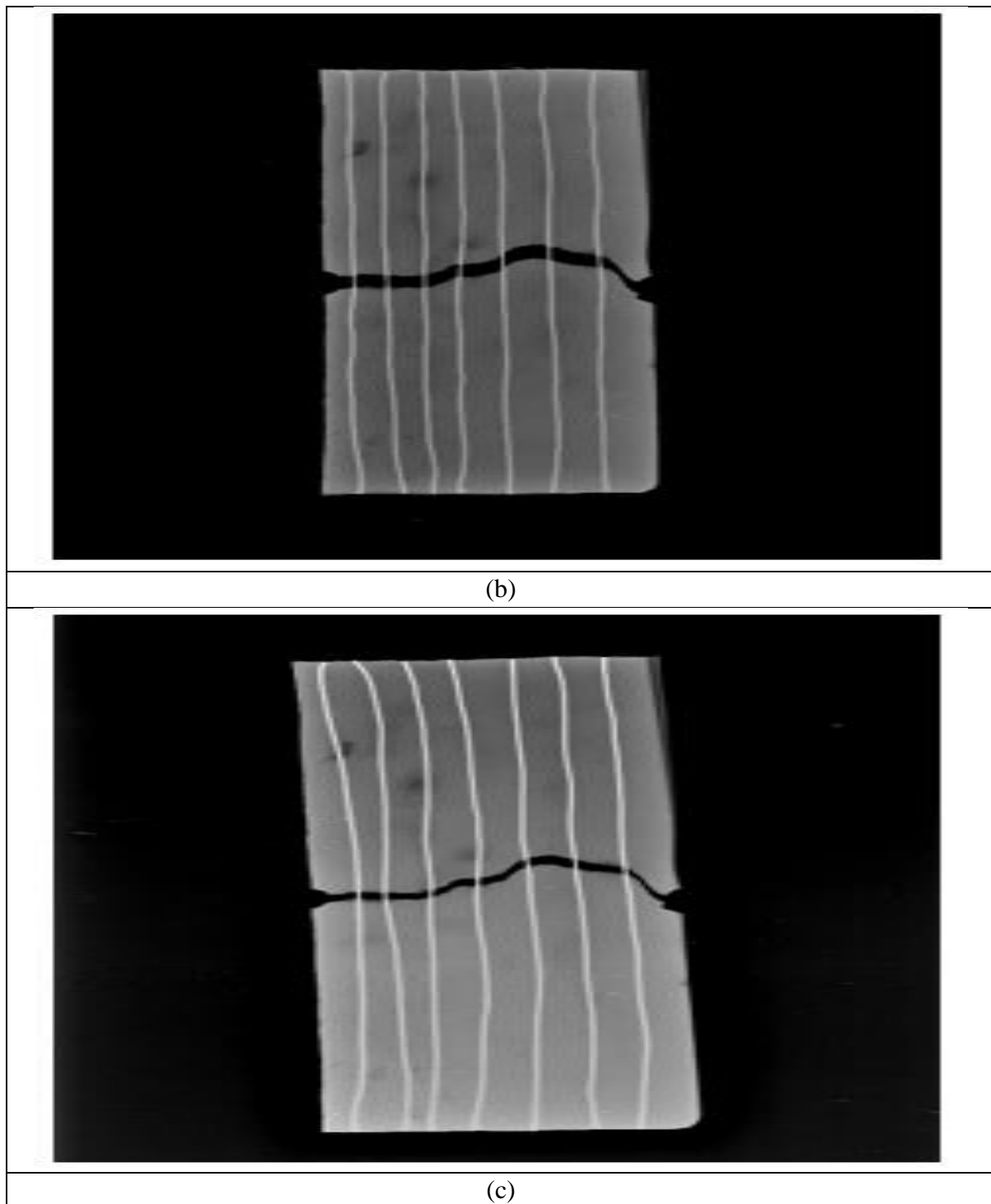
3.4. X-Ray analysis

(a)

(b)

(c)
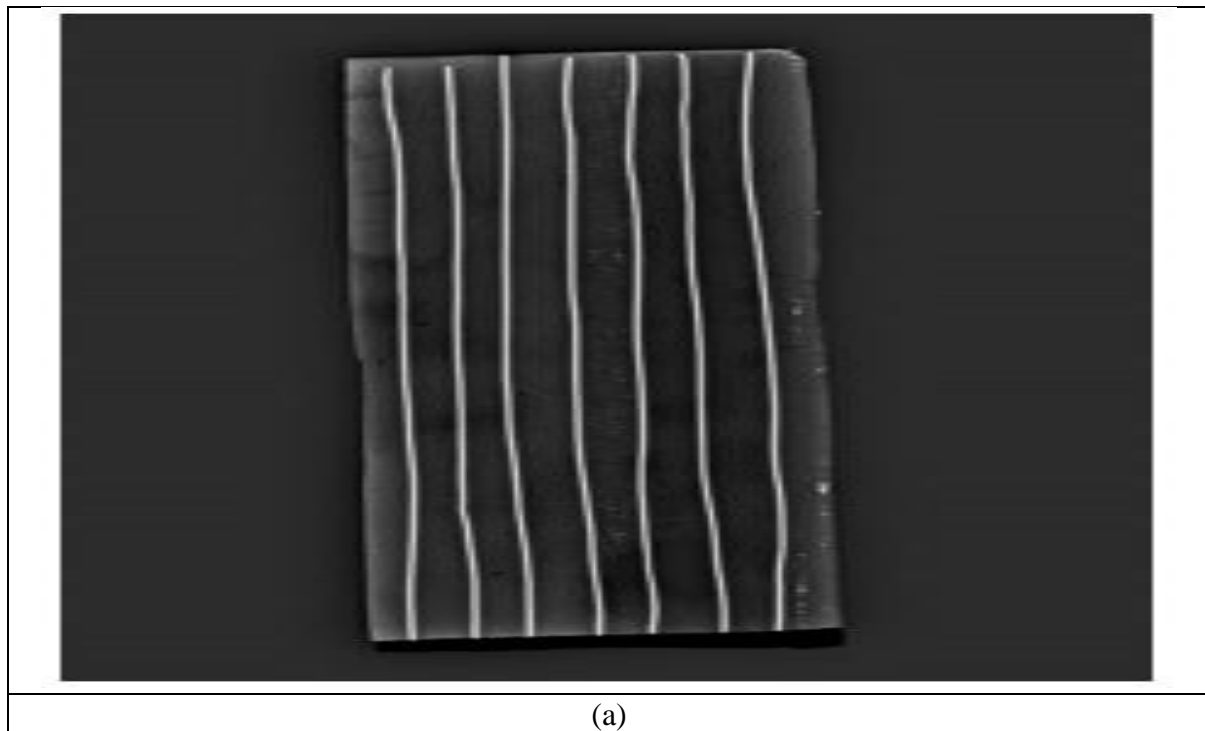
Figure-6. Samples X-ray: (a) Sample before fracture. (b) Sample after fracture. (c) Sample after heat treatment.

Figure-6 shows the samples internal structure. Cu-Mn-Al SMA wires are untouched and it is clear that in the synthesis, due to high temperatures used, wires of Cu-Mn-Al SMA are activated thermally and also from the martensite to austenite phase transition occurs. Fractured composites thermal activation is done by heating the composite sample to 550°C in furnace for heat treatment, holding for 3 hours.

3.5. Vickers hardness test

F - 300 gram, Dwell time – 15 seconds

Table-1. Vickers hardness test results

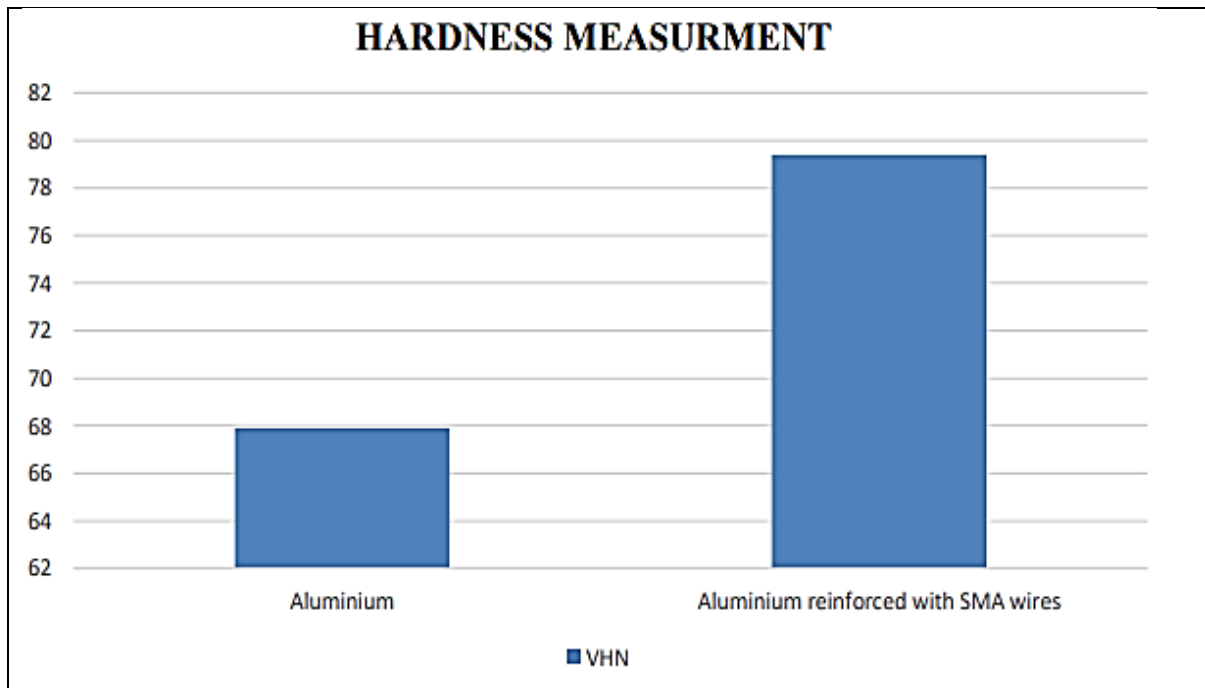| Sr. No.	Specimen	Vickers Hardness Number (VHN)
1	Aluminium	67.9
2	Aluminium reinforced with SMA wires	79.4

Figure-7. Hardness measurement between aluminium specimen and aluminium reinforced with SMA wires specimen

Table-1 shows the Vickers hardness test results and Figure-7 shows the hardness comparison between aluminium specimen and aluminium reinforced with SMA wires specimen. The Vickers hardness is measured on flat surface of the specimen. The hardness of aluminium reinforced with SMA wires specimen is increased when compare with aluminium specimen. By increasing in volume fraction of the reinforcement, the hardness of aluminium reinforced with SMA wire sample is increased. Not only by volume fraction, the hardness increased by increasing the number of SMA wires reinforced with aluminium sample. Another factor that includes in increased hardness is heat treatment techniques.

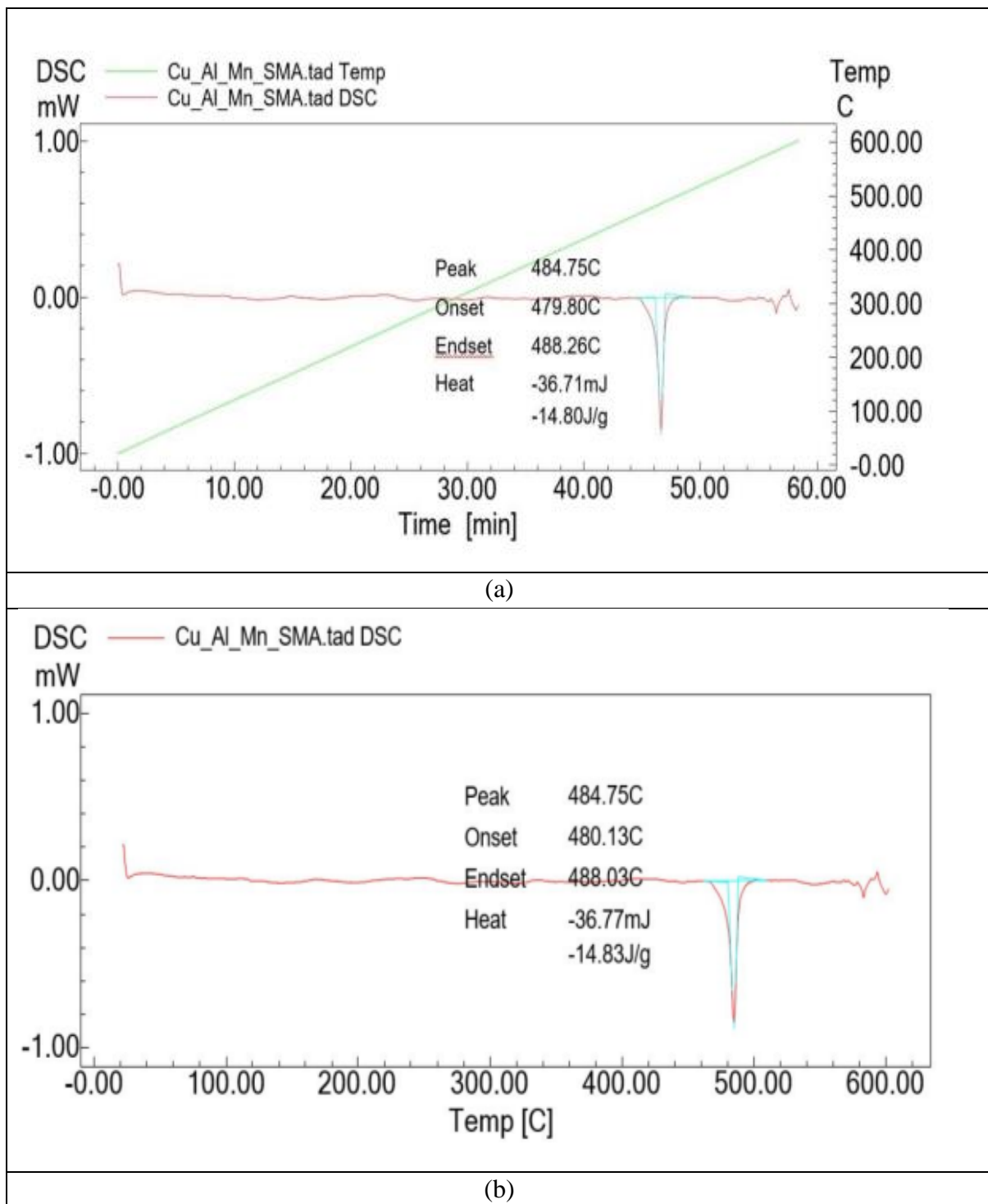## 3.6. Differential scanning calorimetry (DSC) test

(a)

(b)

Figure-8. DSC plot of Cu-Mn-Al Shape memory alloy

An endothermic reaction occurs during heating, transforming martensite to austenite and an exothermic reaction occurs on cooling, resulting in reverse transformation of austenite to martensite. By the respective peaks in plot, these reactions are indicated. With the variations in contents of aluminium and manganese, there is vary in transformation temperatures. The variation in transformation temperatures is mainly attributed to the formation of different types as well as amounts of martensite in the β-phase matrix with the variation in the manganese and

aluminium contents. Figure-8(a) shows the DSC plot between the energy absorption and the time. Figure-8(b) shows the DSC plot between the energy absorption and the temperature. Here the martensite finish temperature i.e. Mf is 479.80°C and the martensite start temperature i.e. MS is 488.26°C and the peak temperature is at 484.75°C.

Table-2. Sample conditions and variation

Number of fibres	Sample size			Test Temperature (°C)	Crack width (mm)	Time to SMA Activation (s)	Crack Closure Duration (s)	Rate of Crack Closure (mm/s)
	Length (cm)	Height (cm)	Width (cm)					
7	15	0.8	5	250	3.55	110	130	0.0273
10	15	0.8	5.5	280	4.1	150	180	0.0227

The samples were tested by varying the number of fibres from 7 to 10. From Table-2, it is observed that the rate of crack closure is almost same. But at higher temperature, with more number, the time for activation and crack closure duration is more may be due to the stiffness of the prepared coupon.

3.7. Shape recovery test

Table-3. Chemical composition and transformation temperature of SMA alloys

Sample number	Composition (wt. %)			Transformation Temperature (K)			
	Cu	Al	Mn	Mf	Ms	As	Af
SMA 1	80.94	10.54	8.52	306	322	325	339
SMA 2	81.10	10.81	8.10	334	358	346	370
SMA 3	83.52	11.36	5.12	370	390	391	416

Table-4. Shape memory strain recovery in different alloys

Sample number	Strain Recovery by SMA (%)
SMA 1	95
SMA 2	89
SMA 3	90

3.8. Experimental data for measurement of SMA activation and crack closure duration

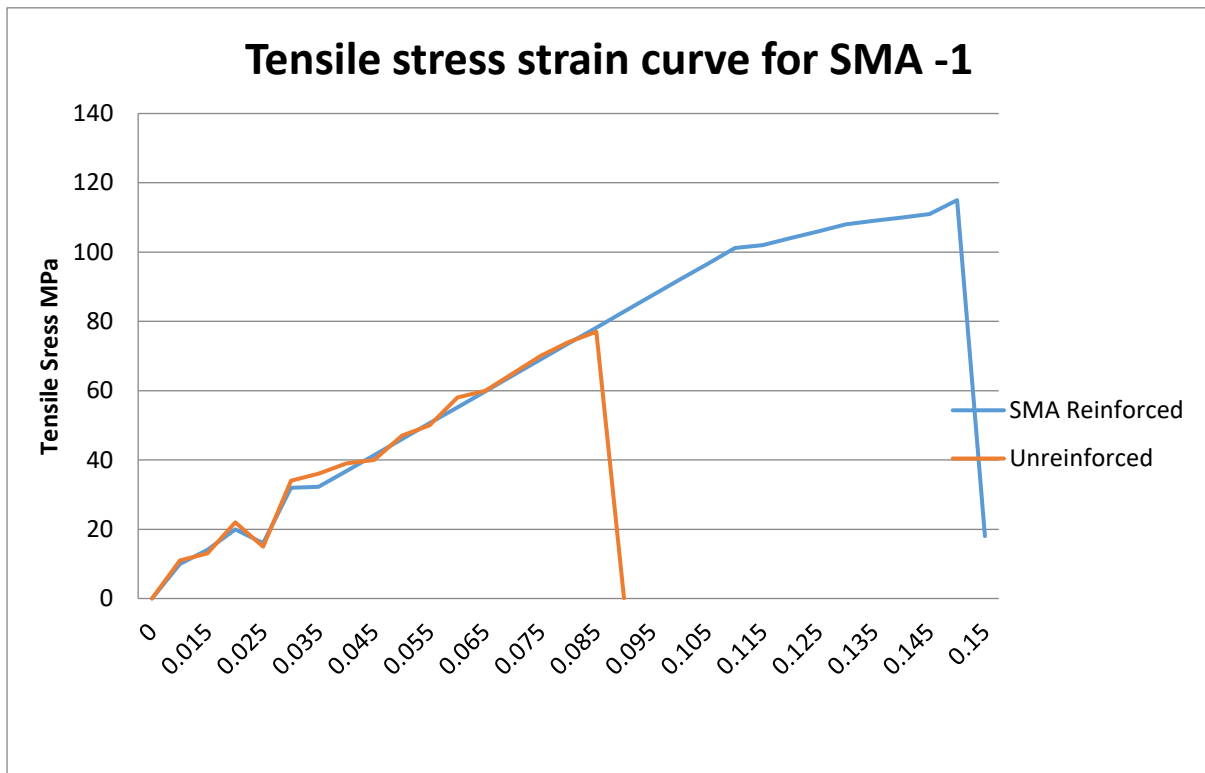| Number of fibers	Diameter of wires reinforced in mm	Sample size			Test temperature (°C)	Crack width (mm)	Time to SMA activation (s)	Crack closure duration (s)	Rate of crack closure (mm/s)
		length (mm)	height (mm)	width (mm)					
8	0.8	80	3	12	69	3.82	240	125	0.0305

Figure-9. Tensile stress–strain curve for SMA-1

4. Conclusion

By ingot metallurgy route, the Cu-Al-Mn SMAs were prepared and tested for SME (Flat and wire specimens). Reinforcement of the Cu-Al-Mn SMA wires in the aluminium matrix. By sample X-Ray analysis, it is ensured that Cu-Al-Mn shape memory alloy wires are untouched during synthesis of aluminium reinforced with SMA wire specimen. The hardness of aluminium reinforced with Cu-Mn-Al SMA wire specimen is 79.4 VHN and unreinforced aluminium sample is 67.9 VHN. There by increase in hardness of SMA wire reinforced specimen due to embedding of Cu-Mn-Al shape memory alloy wires into the aluminium matrix. By self-healing of aluminium matrix reinforced with shape memory alloy wire, there is a reduction in width of crack formed during deformation. It is observed that the rate of crack closure was found to depend on sample dimension rather than the number of wires.

References

1. Abedini M., Ghasemi H.M., Ahmadabadi M.N., Self-healing effect on worn surface of NiTi shape memory alloy, Materials Science and Technology, 2010, 26(3), 285-288, DOI 10.1179/174328409X425308.

2. Ghanbari H., Khalili S.M.R., Farsani R.E., Khalili S., Mahajan P., Experimental investigation on flexural properties of self-healing composites reinforced by shape memory strip, Mechanics of Advanced Materials and Structures, https://doi.org/10.1080/15376494.2019.1601311.

3. Lumley R., Self-Healing in Aluminium Alloys. An Alternative Approach to 20 Centuries of Materials Science, 219-254, 2007, Springer.

4. Mauldin T.C., Kessler M.R., Self-healing polymers and composites, International Materials Reviews, 2010, 55(6), 317-346, DOI 10.1179/095066010X12646898728408.

5. Burton D.S., Gao X., Brinson L.C., Finite element simulation of a self-healing shape memory alloy composite, Mechanics of Materials, 38, 2006, 525–537, doi:10.1016/j.mechmat.2005.05.021.

6. Hassan M.R., Mehrpouya M., Emamian S., Sheikholeslam M.N., Review of Self-Healing Effect on Shape Memory Alloy (SMA) Structures, Advanced Materials Research, 701, 2013, 87-92, doi:10.4028/www.scientific.net/AMR.701.87.

7. Ferguson J.B., Schultz B.F., Rohatgi P.K., Zinc alloy ZA-8/ shape memory alloy self-healing metal matrix composite, Materials Science & Engineering A, http://dx.doi.org/10.1016/j.msea.2014.10.002.

8. Rohatgi P.K., Al-shape memory alloy self-healing metal matrix composite, Materials Science & Engineering A, 619, 2014, 73–76, http://dx.doi.org/10.1016/j.msea.2014.09.050.